AFRL-RX-WP-TP-2011-4367

SUPERPLASTIC BEHAVIOR OF TI-5Al-4V-0.1B ALLOY (PREPRINT)

V. Sinha

UES, Inc.

R. Srinivasan

Wright State University

S. Tamirisakandala

FMW Composite Systems, Inc.

D.B. Miracle

Metals Branch
Metals, Ceramics, and NDE Division

OCTOBER 2011

AIR FORCE RESEARCH LABORATORY
MATERIALS AND MANUFACTURING DIRECTORATE
WRIGHT-PATTERSON AIR FORCE BASE, OH 45433-7750
AIR FORCE MATERIEL COMMAND
UNITED STATES AIR FORCE

REPORT DOCUMENTATION PAGE

Form Approved
OMB No. 0704-0188

1. REPORT DATE *(DD-MM-YY)*	2. REPORT TYPE	3. DATES COVERED *(From - To)*
October 2011	Journal Article Preprint	01 October 2011 – 01 October 2011

4. TITLE AND SUBTITLE
SUPERPLASTIC BEHAVIOR OF TI-5Al-4V-0.1B ALLOY (PREPRINT)

5a. CONTRACT NUMBER
In-house

5b. GRANT NUMBER

5c. PROGRAM ELEMENT NUMBER
62102F

6. AUTHOR(S)
V. Sinha (UES, Inc.)
R. Srinivasan (Wright State University)
S. Tamirisakandala (FMW Composite Systems, Inc.)
D.B. Miracle (AFRL/RXLM)

5d. PROJECT NUMBER
4347

5e. TASK NUMBER
20

5f. WORK UNIT NUMBER
LM10512P

7. PERFORMING ORGANIZATION NAME(S) AND ADDRESS(ES)

UES, Inc.
Dayton, OH 45432-1894

Wright State University
Mechanical and Materials Engineering Department
Dayton OH 45435

FMW Composite Systems, Inc.
Bridgeport, WV 26330

Metals Branch (AFRL/RXLM)
Metals, Ceramics, and NDE Division
Air Force Research Laboratory, Materials and Manufacturing Directorate
Wright-Patterson Air Force Base, OH 45433-7750
Air Force Materiel Command, United States Air Force

8. PERFORMING ORGANIZATION REPORT NUMBER
AFRL-RX-WP-TP-2011-4367

9. SPONSORING/MONITORING AGENCY NAME(S) AND ADDRESS(ES)
Air Force Research Laboratory
Materials and Manufacturing Directorate
Wright-Patterson Air Force Base, OH 45433-7750
Air Force Materiel Command
United States Air Force

10. SPONSORING/MONITORING AGENCY ACRONYM(S)
AFRL/RXLM

11. SPONSORING/MONITORING AGENCY REPORT NUMBER(S)
AFRL-RX-WP-TP-2011-4367

12. DISTRIBUTION/AVAILABILITY STATEMENT
Approved for public release; distribution unlimited.

13. SUPPLEMENTARY NOTES
PAO Case Number: 88ABW 2011-4212; Clearance Date: 01 Aug 2011. Document contains color.
Journal article submitted to *Materials Science and Engineering A.*

14. ABSTRACT
The superplastic behavior of Ti-6Al-4V-0.1B sheet was evaluated. The strain rate sensitivity (m) is ≥ 0.47 in the temperature range 775-900 °C and at strain rate (E)=10-5 to 10-3 s-1. The material exhibits tensile elongations > 200% in the temperature range 725-950 °C at E= 3×10-4 s-1. The optimum superplastic forming temperature is 900 °C, which is similar to conventional Ti-6Al-4V. However, a lower flow stress is needed in the case of Ti-6Al-4V-0.1B. The superplastic deformation mechanism is suggested from estimates of activation energy to be grain boundary sliding (GBS) accommodated by dislocation motion along grain boundaries at E= 10-4 s-1 and is diffusion-controlled dislocation climb at E= 10-3 s-1. Microstructural observations also confirm that GBS is the operating deformation mechanism at 900 °C and E= 3×10-4 s-1.

15. SUBJECT TERMS
titanium alloy, superplasticity, strain rate sensitivity

16. SECURITY CLASSIFICATION OF:			17. LIMITATION OF ABSTRACT:	18. NUMBER OF PAGES	19a. NAME OF RESPONSIBLE PERSON (Monitor)
a. REPORT	b. ABSTRACT	c. THIS PAGE			Jonathan E. Spowart
Unclassified	Unclassified	Unclassified	SAR	26	19b. TELEPHONE NUMBER *(Include Area Code)* N/A

Superplastic Behavior of Ti-6Al-4V-0.1B Alloy

V. Sinha[1,2], R. Srinivasan[3], S. Tamirisakandala[1,4] and D. B. Miracle[1]

[1]Air Force Research Laboratory, Materials and Manufacturing Directorate,
Wright-Patterson AFB, OH 45433, USA

[2]UES, Inc., 4401 Dayton-Xenia Road, Dayton, OH 45432, USA

[3]Mechanical and Materials Engineering Department, Wright State University,
Dayton OH 45435, USA

[4]FMW Composite Systems, Inc., Bridgeport, WV 26330, USA

Abstract

The superplastic behavior of Ti-6Al-4V-0.1B sheet was evaluated. The strain rate sensitivity (m) is ≥ 0.47 in the temperature range 775-900 $^{\circ}$C and at strain rate ($\dot{\varepsilon}$) = 10^{-5} to 10^{-3} s^{-1}. The material exhibits tensile elongations > 200% in the temperature range 725-950 $^{\circ}$C at $\dot{\varepsilon} = 3\times10^{-4}$ s^{-1}. The optimum superplastic forming temperature is 900 $^{\circ}$C, which is similar to conventional Ti-6Al-4V. However, a lower flow stress is needed in the case of Ti-6Al-4V-0.1B. The superplastic deformation mechanism is suggested from estimates of activation energy to be grain boundary sliding (GBS) accommodated by dislocation motion along grain boundaries at $\dot{\varepsilon} = 10^{-4}$ s^{-1} and is diffusion-controlled dislocation climb at $\dot{\varepsilon} = 10^{-3}$ s^{-1}. Microstructural observations also confirm that GBS is the operating deformation mechanism at 900 $^{\circ}$C and $\dot{\varepsilon} = 3\times10^{-4}$ s^{-1}.

Keywords: Titanium alloy, Superplasticity, Strain rate sensitivity

1. INTRODUCTION:

Titanium and its alloys are selected for many critical engineering applications because of their unique combination of properties, such as high specific strength, good fracture/ fatigue resistance and good corrosion resistance. Superplastic forming (SPF) is employed for several Ti-alloys to fabricate intricate and near-net-shape sheet metal components. A large strain rate sensitivity (*m*) and a high elongation are important attributes of a superplastic material. In general, a large *m* is associated with a high elongation [1].

In an early work by Arieli and Rosen [2], it was recognized that a fine grain size favorably influences the superplastic behavior of Ti-6Al-4V (all alloy compositions given in weight percent). Fine grain size (~ 1 μm) and ultra-fine grain size (< 1 μm) Ti-6Al-4V have been examined extensively by several groups in the past decade [3-9]. These prior studies indicate that grain refinement leads to a decrease in superplastic deformation temperature and/ or an increase in strain rate.

TiB and TiC particles in titanium alloy microstructures can inhibit grain growth and thereby contribute to the retention of fine grain size at high temperatures via grain boundary pinning mechanisms. Since a small grain size is beneficial for superplasticity, several studies [10-16] have examined the superplastic behavior of titanium alloys dispersed with TiB or (TiB+TiC). Superplastic deformation of TiB-dispersed Ti-6Al-4V is reported at 900 °C [10-12], which also is an optimum temperature for superplastic deformation of conventional Ti-6Al-4V. Godfrey, *et al.* [10] have shown a lower flow stress for boron-modified Ti-6Al-4V than for conventional Ti-6Al-4V under identical test conditions. Bhat, *et al.* [13] have reported superplasticity of boron-modified Ti-6Al-4V in the β-phase field, where the conventional Ti-6Al-4V is not superplastic due to extensive grain growth. These prior studies on TiB-dispersed Ti-6Al-4V [10-13] have examined materials with B-content ranging from 0.5 to 6.3 wt%. Lu, *et al.* [16] examined (TiB+TiC)-dispersed Ti-6Al-4V and confirmed its superplastic behavior to be similar to conventional Ti-6Al-4V.

Earlier research [17] has reported a substantial grain refinement (~10 ×) with B-addition in as-cast Ti-6Al-4V. Moreover, it was established that the most dramatic grain refinement in as-cast Ti-6Al-4V results from additions of as low as 0.1 wt% B, and further additions of B has little effect on as-cast grain size [17]. It was also shown that as-cast Ti-6Al-4V-0.1B can be directly rolled (without recourse to the ingot-to-billet conversion) into plates and sheets, which is not possible for as-cast Ti-6Al-4V [18]. The improved processability of as-cast Ti-6Al-4V-0.1B was attributed to its finer grain size [18]. In view of the fact that the as-cast grain refinement is caused by as low as 0.1 wt% B and this small amount of B also facilitates the direct rolling of ingots to plates/ sheets, the evaluation of superplastic behavior of Ti-6Al-4V-0.1B sheet is of interest. There are no prior reports on the superplastic behavior of boron-modified Ti-6Al-4V *with B-content < 0.5 wt%.* In the current research, an examination of the superplastic behavior of Ti-6Al-4V-0.1B is undertaken.

2. MATERIAL AND MICROSTRUCTURE:

The ingot of Ti-6Al-4V-0.1B was cast at Flowserve Corporation (Dayton, OH) using the induction skull melting (ISM) approach. The 25-mm thick slices were sectioned from the ingot and cross-rolled along two orthogonal directions to fabricate sheets with a final thickness of 2.15 mm. The rolling start temperature was 954 $^{\circ}$C. Additional details of the sheet fabrication are provided elsewhere [18]. Although the material was rolled in the as-cast condition, no cracking was observed, as described in an earlier study [18].

Two orthogonal sections of the sheet were metallographically polished for microstructural observations. In as-cast Ti-6Al-4V-0.1B, TiB particles are shown to decorate the prior β grain boundaries [17]. In contrast, TiB particles are seen in the rolled material at all the three boundaries: α/α grain boundary, β/β grain boundary and α/β phase boundary (Fig. 1). Similar grain and TiB particle sizes are observed in the two orthogonal sections: Fig. 1 (a) and (b). The average α grain size is ~ 5 μm and the material has ~ 0.5 vol% TiB .

3. EXPERIMENTAL PROCEDURES:

The crystallographic texture was measured using automated electron backscattered diffraction techniques in a scanning electron microscope. The details of this technique are described elsewhere [19]. The step size for the orientation imaging scan was 1 μm, which is smaller than the average α grain size. The scan area was 120 × 200 μm^2. The TSL (Draper, UT, USA) OIM Analysis software was used to plot the basal-plane pole figure.

Room temperature tension tests were conducted in air, using a screw-driven test frame in closed-loop control. The specimen design and nominal dimensions are shown in Fig. 2(a).

High temperature tension tests were conducted in an inert (Ar) atmosphere, using a screw-driven test frame in closed-loop control. The specimen design and nominal dimensions are shown in Fig. 2(b). The crosshead displacement was used to determine the instantaneous gage length and the crosshead speed was adjusted accordingly to run the tests at a particular true strain rate ($\dot{\varepsilon}$).

To determine the superplastic nature of Ti-6Al-4V-0.1B, $\dot{\varepsilon}$ jump tests were carried out. The change in flow stress (σ), as a result of the change in $\dot{\varepsilon}$, was used to determine the *m*-values. Ghosh and Hamilton [1] have discussed $\dot{\varepsilon}$ jump tests in the context of superplastic behavior characterization and have suggested data acquisition at low strains for this purpose. Therefore, in the present work, σ-$\dot{\varepsilon}$ data at true strain (ε) ≤ 0.2 were used to determine the *m*-values under different test conditions.

In addition to the $\dot{\varepsilon}$ jump tests, constant $\dot{\varepsilon}$ (= 3×10^{-4} s^{-1}) tests were carried out to determine the tensile elongation at different test temperatures. The elongation values were used to further confirm the superplasticity in Ti-6Al-4V-0.1B sheet.

4. RESULTS AND DISCUSSION:

4.1 Texture and room temperature tensile properties:

The texture of the rolled sheet of Ti-6Al-4V-0.1B is shown in Fig. 3. Since the sheet was cross-rolled, the pole figure is referred not to the rolling and transverse directions, but the two mutually perpendicular rolling directions are simply labeled '1' and '2' (Fig. 3). The room temperature tensile properties in the two directions are shown in Table I. A higher strength in direction 1 is consistent with the texture shown in Fig. 3, since α-phase is known to have the highest strength in c-orientation [20].

4.2 The *m*-values and tensile elongation at high temperatures:

Table II shows the *m*-values for Ti-6Al-4V-0.1B sheet under different test conditions. An *m*-value of 0.3 and above is generally considered indicative of superplastic behavior [11, 13, 21, 22]. The data in Table II suggest that Ti-6Al-4V-0.1B potentially can be superplastically formed at temperatures as low as 775 $^{\circ}$C and $\dot{\varepsilon}$ in the range of 10^{-5} to 10^{-3} s^{-1}. A higher *m*-value at 900 $^{\circ}$C for the same $\dot{\varepsilon}$-range indicates that the material has better superplasticity at this temperature. Furthermore, the *m*-value at 900 $^{\circ}$C for $\dot{\varepsilon}$ jump of 10^{-3} to 10^{-2} s^{-1} is 0.37 (Table II) and hence, superplastic forming could be carried out at this higher $\dot{\varepsilon}$. Superplastic forming at a higher $\dot{\varepsilon}$ corresponds to a higher productivity [3].

Constant $\dot{\varepsilon}$ (= 3×10^{-4} s^{-1}) tests were run at 900 $^{\circ}$C and the true stress (σ) - true strain (ε) curve for Ti-6Al-4V-0.1B sheet is compared with the flow curve of Ti-6Al-4V in Fig. 4. The flow stress for Ti-6Al-4V-0.1B is lower at a $\dot{\varepsilon}$ of 3×10^{-4} s^{-1} and temperature of 900 $^{\circ}$C. The reason for a lower flow stress of Ti-6Al-4V-0.1B is currently unclear. However, this is consistent with the results of Godfrey *et al.* [10], where a lower flow stress was reported in Ti-6Al-4V-0.5B than in conventional Ti-6Al-4V. Since the flow stress is directly related to the gas pressure required to superplastically form a sheet [3], a lower gas pressure would be sufficient for a Ti-6Al-4V-0.1B sheet than for a Ti-6Al-4V sheet. Furthermore, a material exhibiting an elongation $\geq$ 200% potentially can be considered for superplastic forming [3, 13]. The elongation at 900 $^{\circ}$C and $\dot{\varepsilon}$ = 3×10^{-4} s^{-1} is 460% (ε = 1.72), and this also suggests that the Ti-6Al-4V-0.1B sheet is suitable for superplastic forming.

During a superplastic forming operation, a metal sheet is typically deformed not in a uniaxial fashion, but the stress state is biaxial. The importance of biaxial stress state in superplastic forming is recognized in earlier studies (e.g. [1]). In view of this, the tensile tests of Ti-6Al-4V-0.1B sheet were also conducted along direction 2. The tensile elongation was determined as a function of temperature at the constant $\dot{\varepsilon}$ = 3×10^{-4} s^{-1} (Fig. 5). The dotted line in Fig. 5 corresponds to an elongation of 200%, which is the cut-off for superplastic forming. Fig. 5 shows that the elongation is $\geq$ 200% at temperatures in the range 725 – 950 $^{\circ}$C and therefore, SPF potentially can be carried out in this temperature range at a $\dot{\varepsilon}$ = 3×10^{-4} s^{-1}. Furthermore, the highest elongation (exceeding 646%) is observed at 900 $^{\circ}$C and it is the optimum temperature for SPF. This is consistent with the *m*-values described above (Table II). The elongation in direction 2 at 900 $^{\circ}$C is higher than in direction 1.

4.3 Superplastic deformation mechanism:

The activation energy for a particular deformation process gives an idea about the rate-controlling mechanism. Assuming that deformation during high temperature tension tests is thermally activated, the strain rate can be expressed as [4]:

$$\dot{\varepsilon} = A\,\sigma^{n} \exp(-Q/RT) \quad \text{----------} \quad (1)$$

where A is a frequency factor, n (=1/m) is the stress exponent, Q is the activation energy, R is the universal gas constant, and T is the absolute temperature. For a fixed $\dot{\varepsilon}$, equation (1) can be re-arranged to obtain an expression for Q:

$$Q = n\,R\,\frac{\partial \ln\sigma}{\partial\,(1/T)} \quad \text{----------} \quad (2)$$

Therefore, the activation energy of the deformation process can be estimated from the slope of a log σ *versus* 1/T plot for a given $\dot{\varepsilon}$.

Equation (2) is valid strictly for conditions where m is independent of T. Although the m-value of Ti-6Al-4V-0.1B sheet varies with a change of temperature (Table II), an average m was used to obtain a first order approximation for Q. There is only ±15% variation about the average value of m at $\dot{\varepsilon} = 5\times10^{-4}$ s^{-1} and ε = 0.1 (Table II). Therefore, use of an average m is expected to give reasonable estimates of Q.

Fig. 6 shows the plot of log σ *versus* 1/T at constant $\dot{\varepsilon}$ of 10^{-4} and 10^{-3} s^{-1} for Ti-6Al-4V-0.1B sheet. The estimated value of Q at $\dot{\varepsilon} = 10^{-4}$ s^{-1} is 207 kJ/mol and it is 155 kJ/mol at $\dot{\varepsilon} = 10^{-3}$ s^{-1}. Arieli and Rosen [2] have reported an apparent activation energy of 188 kJ/mol for superplastic deformation of Ti-6Al-4V and proposed a mechanism of grain boundary sliding (GBS) accommodated by dislocation motion (climb) along grain boundaries. A similar value of Q at $\dot{\varepsilon} = 10^{-4}$ s^{-1} in the present work suggests that deformation *via* GBS accommodated by dislocation motion along grain boundaries may be operating. On the other hand, at $\dot{\varepsilon} = 10^{-3}$ s^{-1} the value of Q is closer to that for volume diffusion in α-titanium (150 kJ/mol) [23], and also volume diffusion as well as grain boundary diffusion in β-titanium (153 kJ/mol) [23, 24]. Q is reported to have the same value for volume diffusion and grain boundary diffusion in β-titanium [23]. Therefore, we suggest that the operating deformation mechanism shifts toward diffusion leading to dislocation climb in the α and/ or β phase(s), and/ or along the grain boundaries in the β-phase at a $\dot{\varepsilon} = 10^{-3}$ s^{-1}.

The microstructure of superplastically deformed Ti-6Al-4V-0.1B is shown in Fig. 7. The α-grain size is ~ 15 μm and a comparison with starting microstructure (Fig. 1) suggests that grain coarsening does occur during superplastic deformation. A similar change in β-grain size is observed. Moreover, the β phase becomes more continuous during superplastic deformation (compare Fig. 7 with Fig. 1). The backscattered electron (BSE) image is shown in Fig. 7(a), whereas Fig. 7(b) shows the secondary electron (SE) image of the same area. Although cavities have a darker shade than TiB in the BSE image, it is easier to differentiate between the two in the SE image as cavities are surrounded by bright regions in this image (Fig. 7(b)). It is evident that

cavitation occurs at phase/ grain boundaries. Furthermore, cavities are observed both at TiB/(α or β) interfaces and away from TiB. This suggests that TiB is not the preferential site for cavitation. We propose that with continued deformation, resistance to GBS develops (possibly due to the grain coarsening as well as any dislocation networks at the grain/ phase boundaries) and it eventually leads to cavitation at grain/ phase boundaries. With further deformation, the cavities link up and finally lead to specimen failure. Therefore, the occurrence of cavities at grain/ phase boundaries is a manifestation of GBS during superplastic deformation of Ti-6Al-4V-0.1B. This is consistent with the deformation mechanism suggested above from the activation energy consideration.

There are two competing effects of TiB in the microstructure: (i) TiB pins the grain/ phase boundaries at high temperatures in accordance with the Zener model [25] and thereby, reduces the grain growth. This is expected to be beneficial for superplasticity. (ii) TiB is present mostly at grain/ phase boundaries and therefore, is likely to hinder the grain boundary sliding during high temperature deformation. Since the operating deformation mechanism for superplasticity is GBS, it is expected that this effect is detrimental for SPF. In view of the results of current research, we propose that these two effects balance each other and the net outcome is that the SPF characteristics of Ti-6Al-4V-0.1B sheet are similar to the conventional Ti-6Al-4V.

5. SUMMARY AND CONCLUSIONS:

In this research, the superplastic behavior of Ti-6Al-4V-0.1B sheet was examined. The sheet was fabricated via cross-rolling of as-cast ingot. The conclusions are as follows:
(i) The *m*-values, determined from $\dot{\varepsilon}$ jump tests in tension indicate that the material is superplastic at $\dot{\varepsilon} = 10^{-5}$ to 10^{-3} s^{-1} and in the temperature range 775-900 $^{\circ}$C.
(ii) Constant $\dot{\varepsilon}$ tension tests further confirm the superplastic behavior of Ti-6Al-4V-0.1B sheet at $\dot{\varepsilon} = 3\times10^{-4}$ s^{-1} in the temperature range 725-950 $^{\circ}$C.
(iii) The optimum temperature for superplastic forming is 900 $^{\circ}$C. At this temperature, the material can be superplastically deformed at $\dot{\varepsilon}$ as high as 10^{-2} s^{-1}.
(iv) The optimum superplastic forming temperature for Ti-6Al-4V-0.1B is similar to conventional Ti-6Al-4V. However, the flow stress is lower for Ti-6Al-4V-0.1B.
(v) The Ti-6Al-4V-0.1B sheet behaves superplastically along each of the two cross-rolled directions.
(vi) Estimation of the activation energy indicates that superplastic deformation occurs via GBS accommodated by dislocation motion along grain boundaries at $\dot{\varepsilon} = 10^{-4}$ s^{-1}, whereas it occurs via diffusion-controlled dislocation climb at $\dot{\varepsilon} = 10^{-3}$ s^{-1}.
(vii) Microstructural observations confirm superplastic deformation via GBS at 900 $^{\circ}$C and at $\dot{\varepsilon} = 3\times10^{-4}$ s^{-1}.

Acknowledgments:
This research was supported by Air Force Research Laboratory, Materials and Manufacturing Directorate (Contract # FA9650-04-D-5233). The authors thank Mike Scott (UES, Inc.) for help with running the high temperature tension tests. The Ti-6Al-4V-0.1B sheets used in this study were fabricated in collaboration with Scott Reed (Flowserve) and Oscar Yu (RTI) under EMTEC Project CT-86.

References:

1. A.K. Ghosh and C. H. Hamilton, Metallurgical Transactions A, Vol. 13A, pp. 733-743,1982.

2. A. Arieli and A. Rosen, Metallurgical and Materials Transactions A, Vol. 8A, pp. 1591-1596, 1977.

3. P.N. Comley, Journal of Materials Engineering and Performance, Volume 13(6), pp. 660-664, December 2004.

4. Y.G. Ko, C.S. Lee, D.H. Shin, and S.L. Semiatin, Metallurgical and Materials Transactions A, Vol. 37A, pp. 381-391, 2006.

5. Y.G. Ko, W.G. Kim, C.S. Lee, and D.H. Shin, Materials Science and Engineering A, 2005, vols. 410–411, pp. 156-59.

6. A.V. Sergueeva, V.V. Stolyarov, R.Z. Valiev, A.K. Mukherjee, Materials Science and Engineering A323 (2002) 318–325.

7. S.N. Patankar, J.P. Escobedo, D.P. Field, G. Salishchev, R.M. Galeyev, O.R. Valiakhmetov, F.H. (Sam) Froes, Journal of Alloys and Compounds 345 (2002) 221–227.

8. A.V. Sergueeva, V.V. Stolyarov, R.Z. Valiev, A.K. Mukherjee, Scripta Materialia 43 (2000) 819–824.

9. G.A. Salishchev, R.M. Galeyev, O.R. Valiakhmetov, R.V. Safiullin, R.Y. Lutfullin, O.N. Senkov, F.H. Froes, and O.A. Kaibyshev, Journal of Materials Processing Technology, Vol 116, 2001, pp. 265-268.

10. T.M.T. Godfrey, A. Wisbey, A. Brown, R. Brydson, and C. Hammond, Materials Science and Technology, Vol 16, 2000, pp. 1302-1308.

11. M. Kobayashi, K. Funami, S. Suzuki, and C. Ouchi, Materials Science and Engineering A243 (1998) 279–284.

12. K. Funami, M. Kobayashi, S. Suzuki, and C. Ouchi, Materials Science Forum Vols. 243-245 (1997) pp 515-520.

13. R.B. Bhat, S. Tamirisakandala, and D.B. Miracle, Journal of Materials Engineering and Performance, Volume 13(6), pp. 653-659, December 2004.

14. M.M. Wang, W.J. Lu, J.N. Qin, D. Zhang, B. Ji, and F. Zhu, Scripta Materialia 53 (2005), pp. 265-270.

15. M.M. Wang, W.J. Lu, J.N. Qin, D. Zhang, B. Ji, and F. Zhu, Scripta Materialia 54 (2006), pp. 1955-1959.

16. J. Lu, J. Qin, Y. Chen, Z. Zhang, W. Lu, and D. Zhang, Journal of Alloys and Compounds 490 (2010) 118–123.

17. S. Tamirisakandala, R.B. Bhat, J.S. Tiley, and D.B. Miracle, Scripta Materialia 53 (2005) pp. 1421–1426.

18. R. Srinivasan, S. Tamirisakandala, D. Miracle, K-O Yu, V. Sinha, F. Sun, M. Bennett, and J.M. Scott, "Production of Plates and Sheets from As-Cast Ti-6Al-4V via Boron Modification", in: Ti-2007 Science and Technology: Proceedings of the 11th World Conference on Titanium, M. Niinomi, S. Akiyama, M. Ikeda, M. Hagiwara, and K. Maruyama (Editors), The Japan Institute of Metals, pp. 977-980, 2007.

19. S.I. Wright: in Electron Backscatter Diffraction in Materials Science, A.J. Schwartz, M. Kumar, and B.L. Adams, ed., Kluwer Academic/Plenum Publishers, New York, NY, 2000, pp. 51-64.

20. J.C. Williams, R.G. Baggerly, and N.E. Paton, Metallurgical and Materials Transactions A, Vol. 33A, pp. 837-850, 2002.

21. W.A. Backofen, I.R. Turner, D.H. Avery, Trans. ASM 57 (1964) 980.

22. J. Sieniawski and M. Motyka, Journal of Achievements in Materials and Manufacturing Engineering, Volume 24, Issue 1, September 2007, pp. 123-130.

23. Z.X. Guo and N. Ridley: Mater. Sci. Technol., 1987, vol. 3, pp. 945-53.

24. N.E.W. De Reca and C.M. Libanati, Acta Metallurgica 16 (1968) pp. 1297–1305.

25. C. Zener, see C. S. Smith, Trans. Metall. Soc. A.I.M.E., Vol. 175, pp. 47-48 (1948).

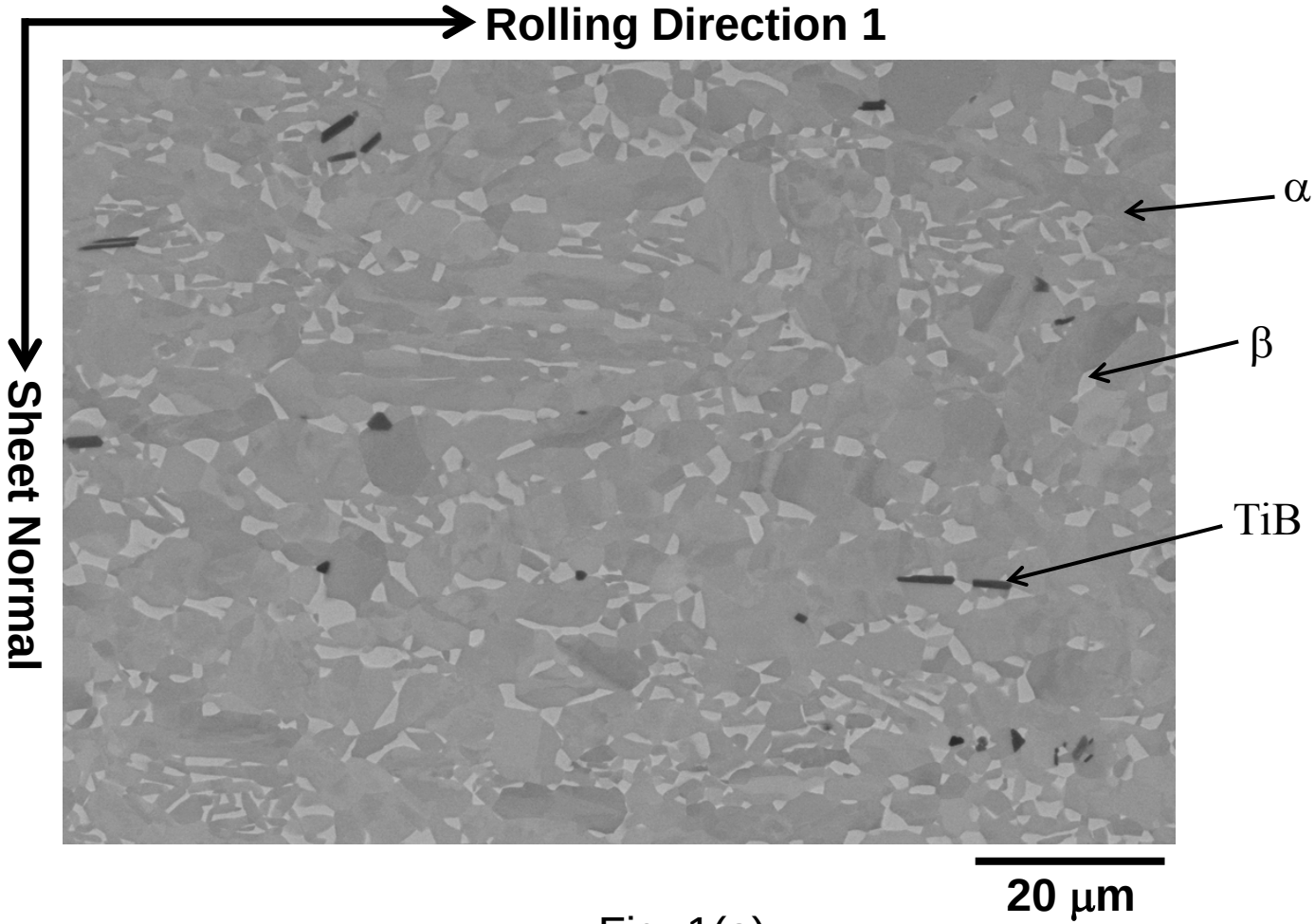

Fig. 1(a)

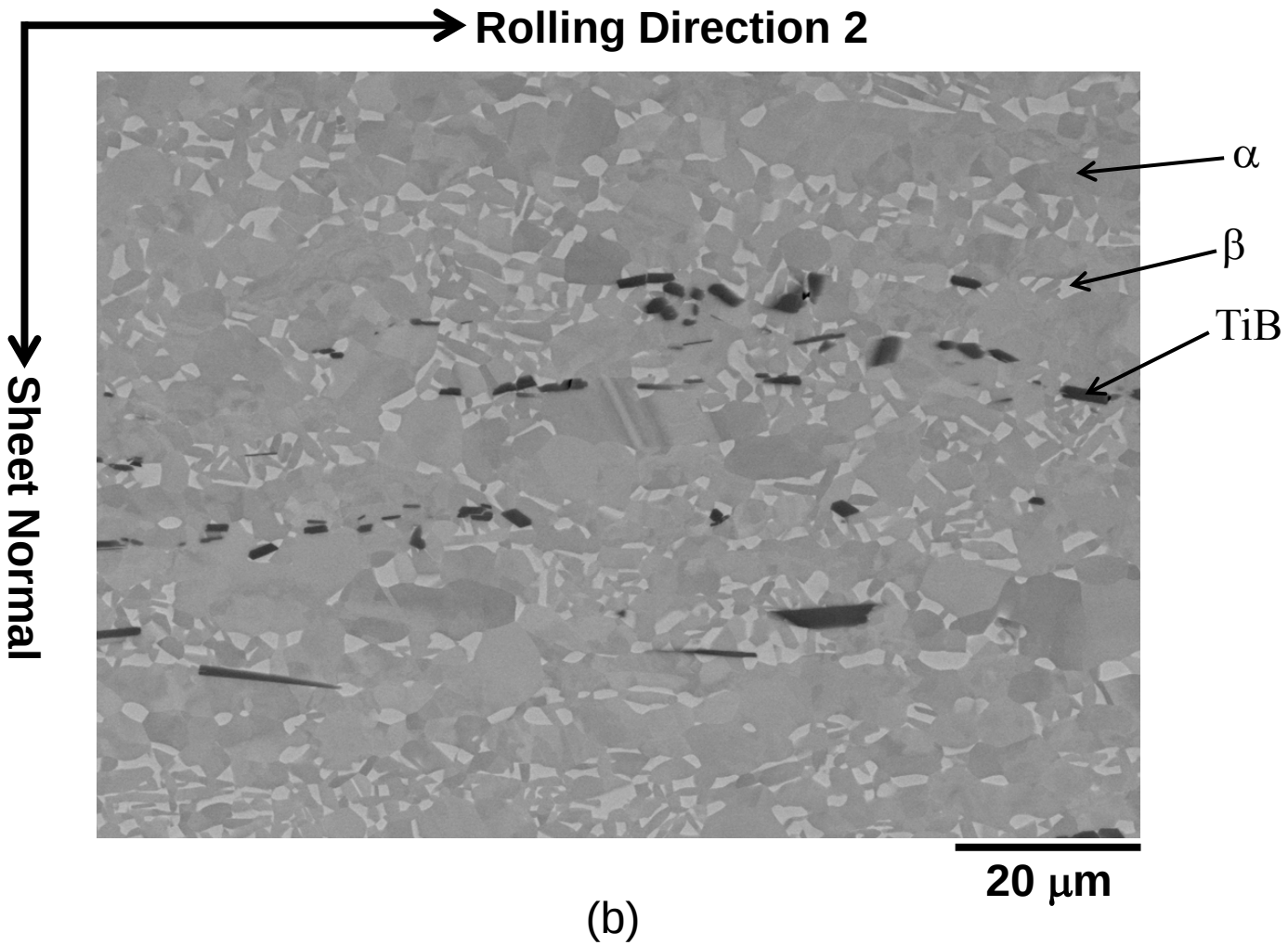

Fig. 1: Microstructure of the Ti-6Al-4V-0.1B sheet: backscattered electron images acquired in an SEM. Plane of image contains sheet normal and rolling direction 1 in (a) , whereas it contains sheet normal and rolling direction 2 in (b).

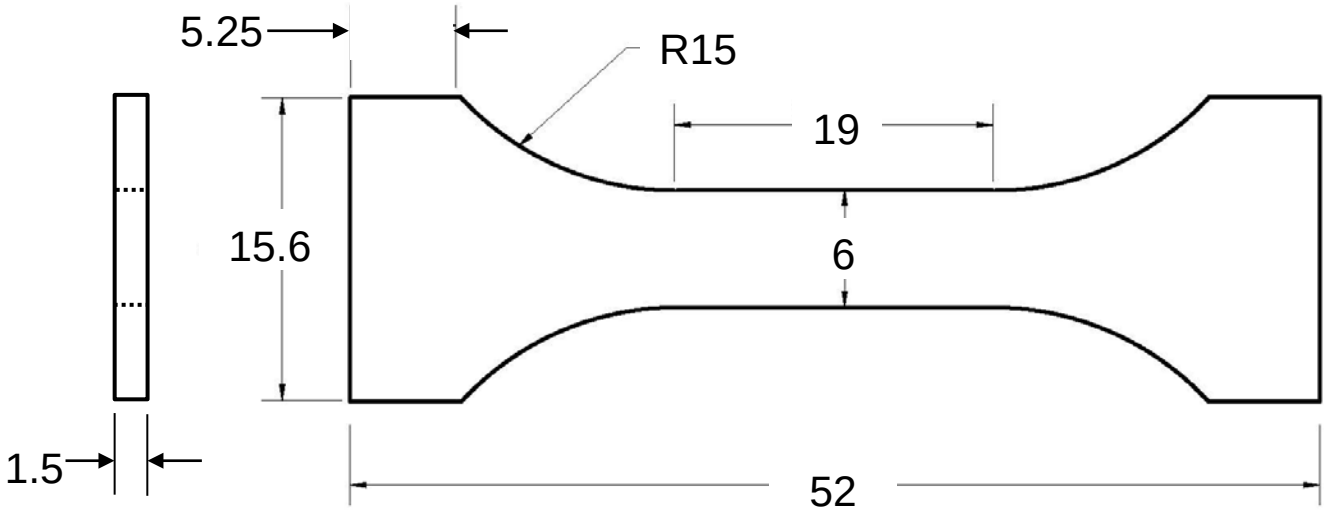

Dimensions are in mm.

Fig. 2(a)

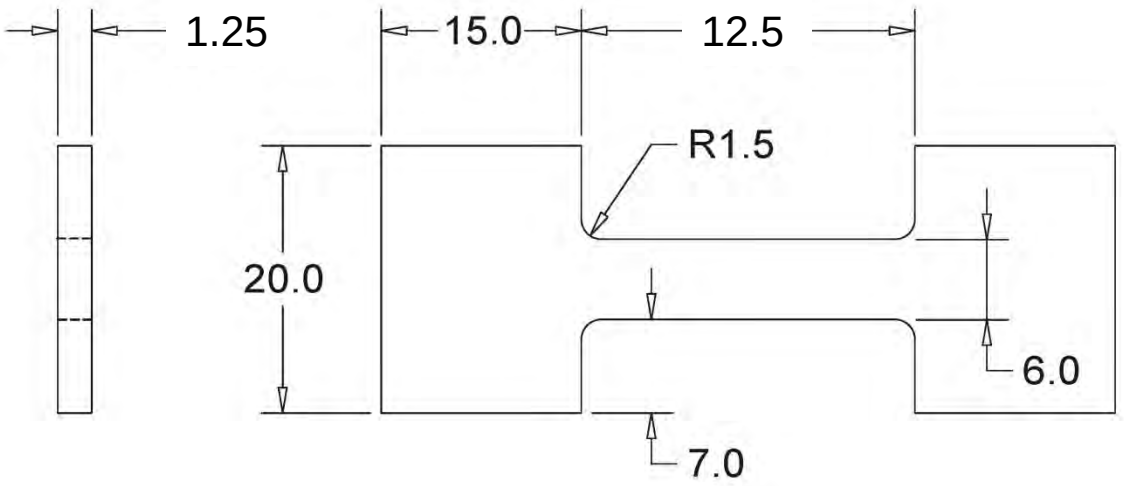

(b)

Fig. 2: Design of specimens for (a) room temperature, and (b) high-temperature tension tests.

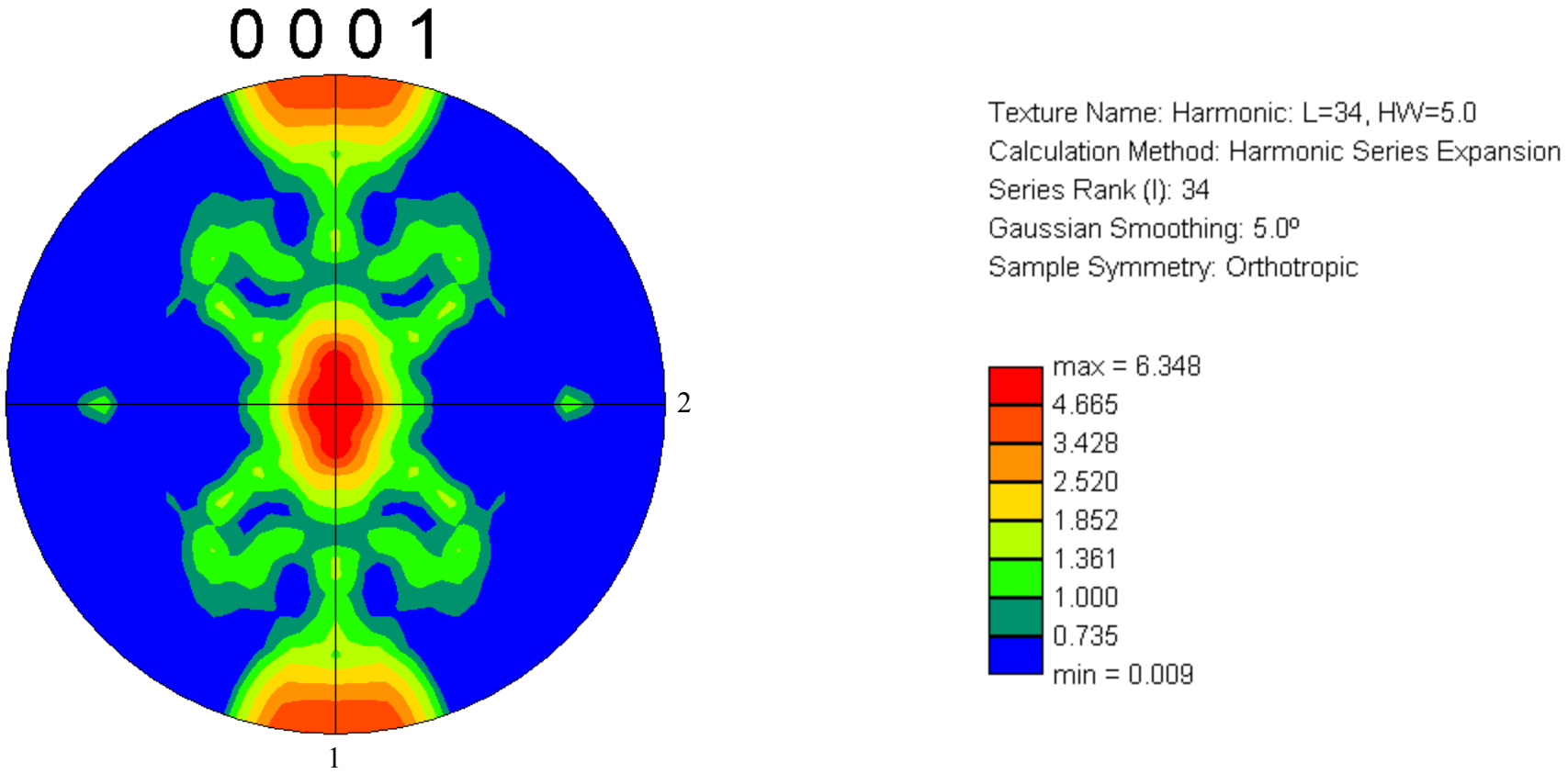

Fig. 3: Basal plane pole figure for the Ti6Al-4V-0.1B sheet. '1' and '2' indicate the two cross-rolling directions.

TABLE I: Room-temperature tensile properties of Ti-6Al-4V-0.1B sheet

Loading axis orientation	Yield Strength (MPa)	Ultimate Tensile Strength (MPa)	Elongation (%)
Direction 1	1035	1081	15.9
Direction 2	950	1033	18.4

TABLE II: Strain rate sensitivity of Ti-6Al-4V-0.1B sheet

Temperature (˚C)	Strain	Strain Rate* (s^{-1})	*m*
775	0.05	5×10^{-5}	0.71
	0.1	5×10^{-4}	0.47
825	0.05	5×10^{-5}	0.69
	0.1	5×10^{-4}	0.54
900	0.1	5×10^{-5}	0.75
	0.1	5×10^{-4}	0.63
	0.2	5×10^{-3}	0.37

*A strain rate of 5×10^{-5} s^{-1} corresponds to a $\dot{\varepsilon}$-jump from 10^{-5} to 10^{-4} s^{-1}, 5×10^{-4} s^{-1} corresponds to a $\dot{\varepsilon}$-jump from 10^{-4} to 10^{-3} s^{-1}, and 5×10^{-3} s^{-1} corresponds to a $\dot{\varepsilon}$-jump from 10^{-3} to 10^{-2} s^{-1}. Tensile axis was along direction 1.

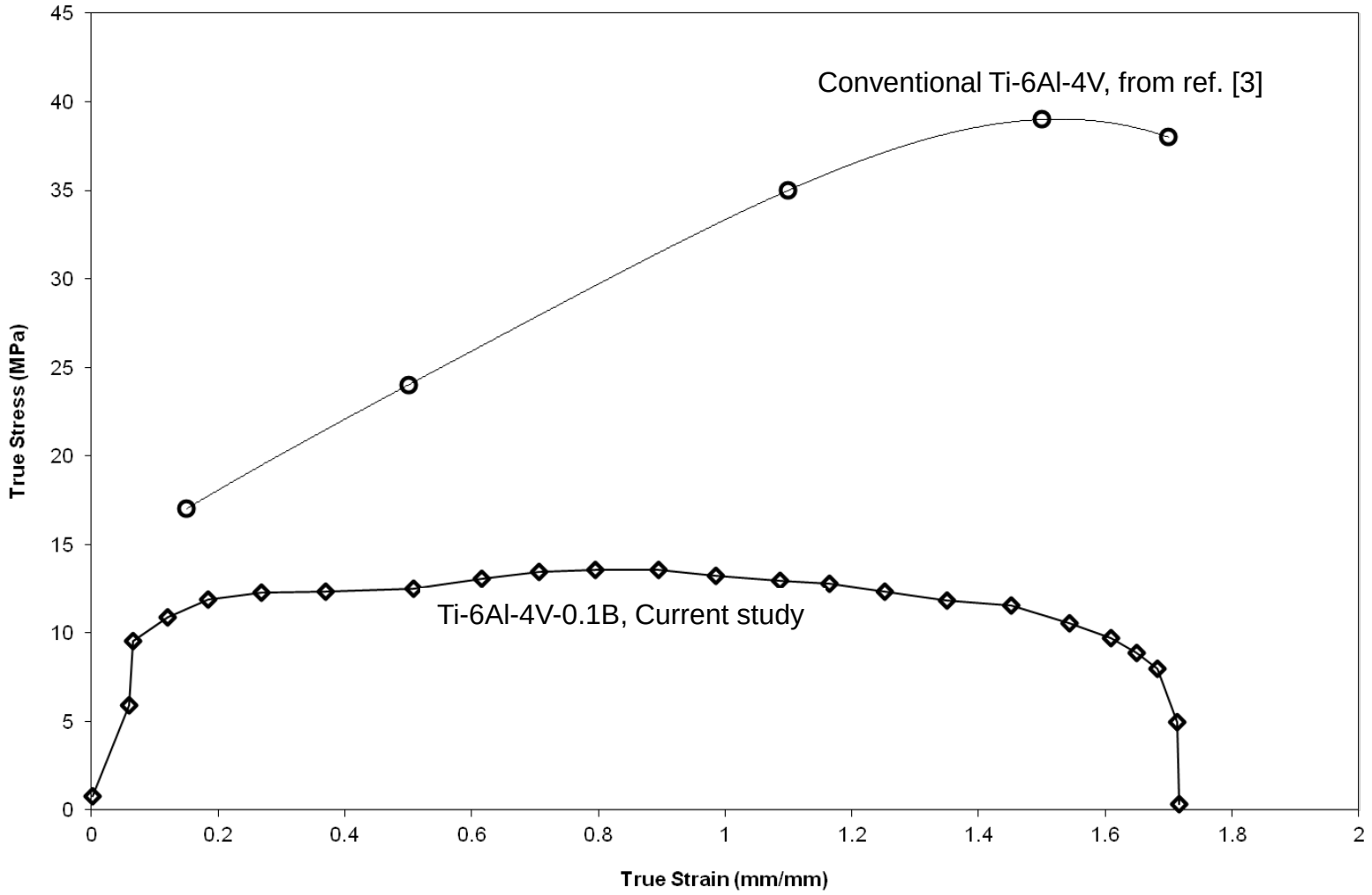

Fig. 4: True stress- true strain curves for Ti-6Al-4V-0.1B and conventional Ti-6Al-4V alloys. Test temperature = 900 ˚C and strain rate = 3×10^{-4} s^{-1}.

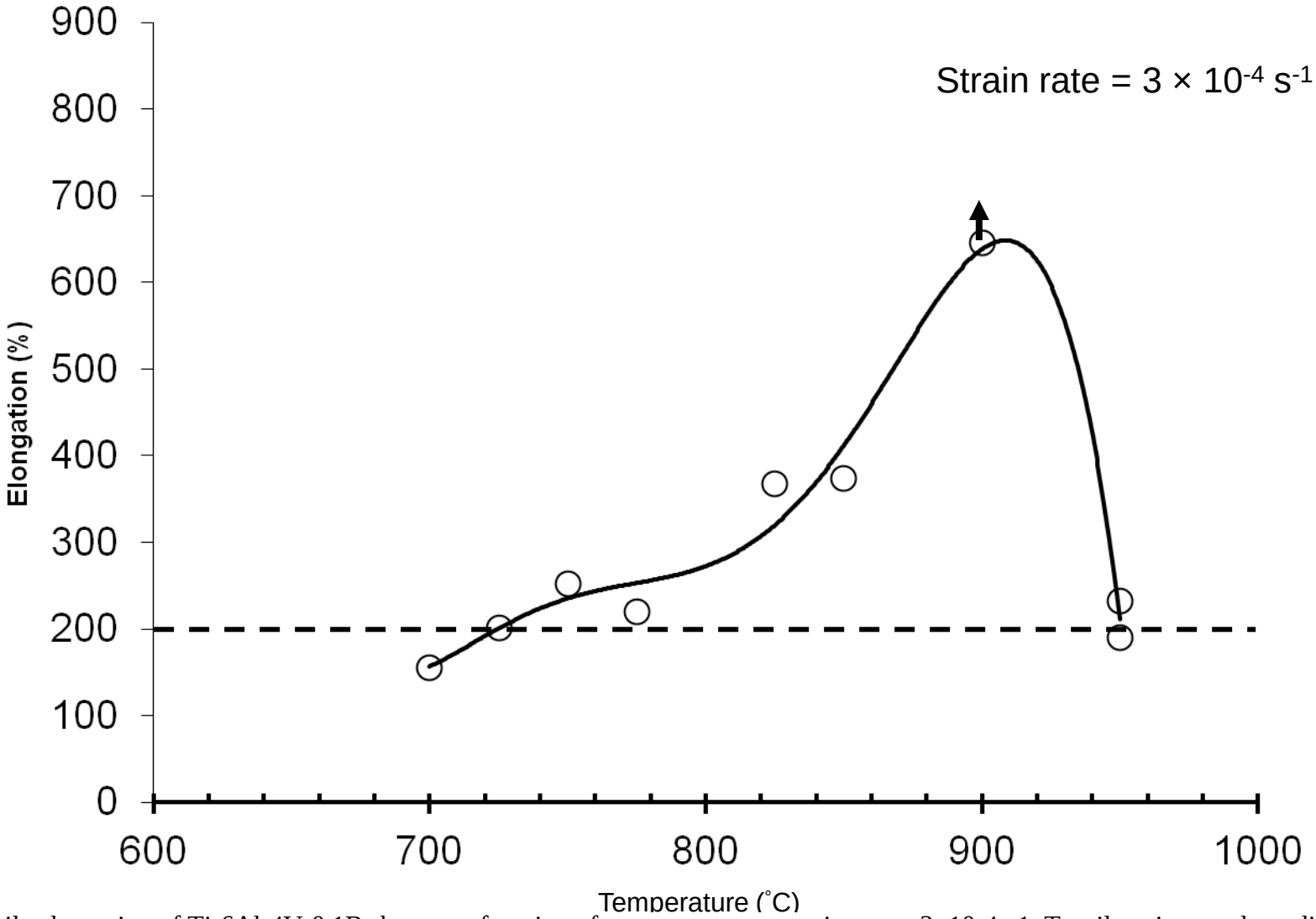

Fig. 5: Tensile elongation of Ti-6Al-4V-0.1B sheet as a function of temperature at a strain rate = 3×10-4s-1. Tensile axis was along direction 2.

The specimen at 900 °C did not fail at the maximum crosshead displacement of the test frame.

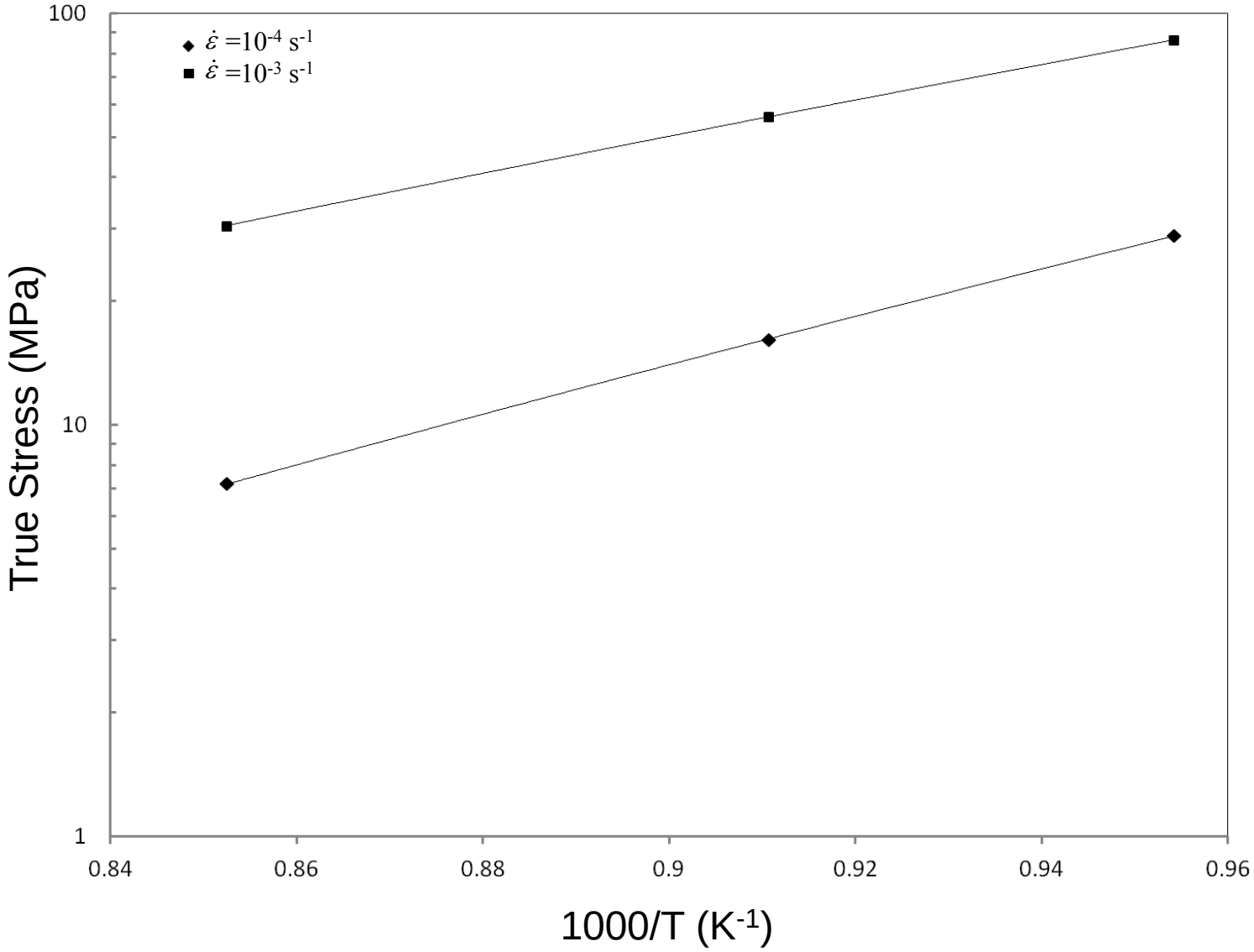

Fig. 6: Plot of log σ vs 1/T at $\dot{\varepsilon}$ of 10^{-4} and 10^{-3} s^{-1}. The slope is used to calculate the activation energy of the deformation process.

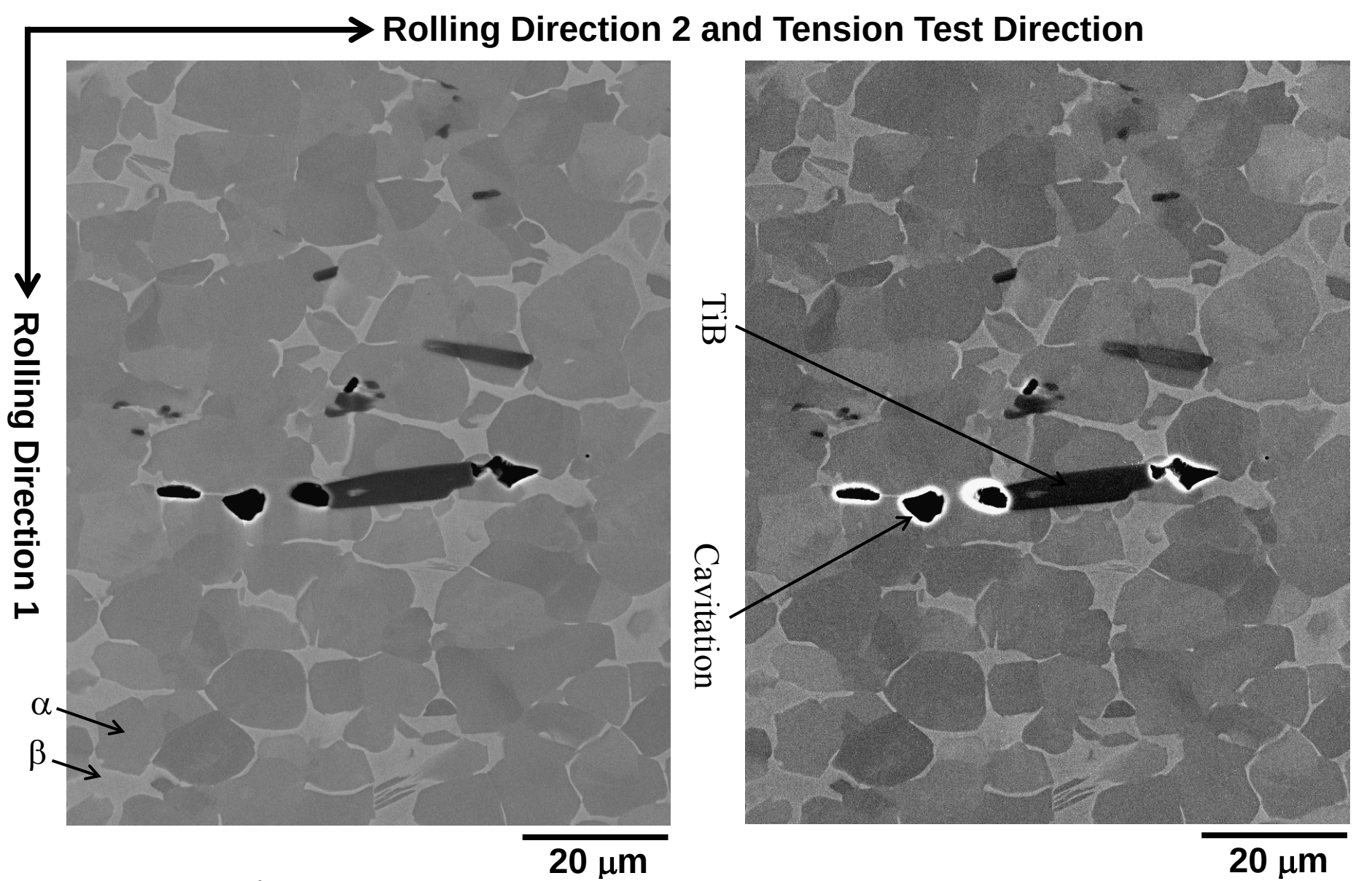

Fig. 7: Microstructure of the high-temperature tension-tested Ti-6Al-4V-0.1B sheet. Test temperature = 900 °C and strain rate = 3×10-4s-1. (a) Backscattered electron image, and (b) secondary electron image.